

# Power law behavior for the zigzag transition in a Yukawa cluster

T. E. Sheridan\* and Andrew L. Magyar<sup>†</sup>

*Department of Physics and Astronomy,  
Ohio Northern University, Ada, OH 45810*

## Abstract

We provide direct experimental evidence that the one-dimensional (1D) to two-dimensional (2D) zigzag transition in a Yukawa cluster exhibits power law behavior. Configurations of a six-particle dusty (complex) plasma confined in a biharmonic potential well are characterized as the well anisotropy is reduced. When the anisotropy is large the particles are in a 1D straight line configuration. As the anisotropy is decreased the cluster undergoes a zigzag transition to a 2D configuration. The measured dependence of cluster width on anisotropy is well described by a power law. A second transition from the zigzag to an elliptical configuration is also observed. The results are in very good agreement with a model for particles interacting through a Yukawa potential.

arXiv:1001.0753v1 [physics.plasm-ph] 5 Jan 2010

---

\*Electronic address: t-sheridan@onu.edu

<sup>†</sup>Present address: Department of Physics, Penn State University, University Park, PA 16802

Plasma is a quasi-neutral gas that contains electrons, ions and (often) neutral atoms and which exhibits collective behavior [1]. A dusty (complex) plasma is a systems of interacting microscopic dust particles immersed in a standard electron-ion plasma. For typical laboratory conditions, dust particles acquire a net charge  $q < 0$  from the electron and ion currents. The Coulomb interaction between the charged dust particles is shielded by the response of the free charge in the plasma. In the plane of a two-dimensional cluster, the inter-particle potential is well approximated by a Yukawa (i.e., Debye or shielded Coulomb) potential [2]

$$V(r) = \frac{1}{4\pi\epsilon_0} \frac{q}{r} e^{-r/\lambda_D}, \quad (1)$$

where  $\lambda_D$  is the Debye screening length. An unshielded Coulomb interaction is recovered as  $\lambda_D \rightarrow \infty$ . Dusty plasma is an exceptional experimental system for examining the static and dynamic properties of Yukawa clusters—small clusters of particles interacting through a Yukawa potential.

In laboratory experiments the dusty plasma is usually confined, typically through a combination of gravitational and electrical forces. Monodisperse microspheres may then form strongly-coupled one-dimensional (1D) [3–5], two-dimensional (2D) [6–8] or even three-dimensional systems [9]. The general 2D potential well is biharmonic for small displacements from the potential energy minimum [10–12]. A dusty plasma confined in a 2D biharmonic well may be either in a 1D straight line configuration, or a 2D configuration, where the transition from 1D to 2D states is via the zigzag instability [10, 11, 13–15].

A cold 2D dusty plasma can be modeled [10, 12, 16] by assuming  $n$  identical particles with mass  $m$  and charge  $q$ , where the  $i$ th particle is at  $(x_i, y_i)$ . The potential energy  $U$  of a configuration  $\{x_i, y_i\}$  is given by the sum of the particles' potential energy with respect to the biharmonic well plus the sum of the potential energy for each pair-wise interaction,

$$U = \sum_{i=1}^n \frac{1}{2} m (\omega_x^2 x_i^2 + \omega_y^2 y_i^2) + \sum_{i=1}^n \sum_{j>i}^n \frac{1}{4\pi\epsilon_0} \frac{q^2}{r_{ij}} e^{-r_{ij}/\lambda_D}, \quad (2)$$

where  $r_{ij} = \sqrt{(x_i - x_j)^2 + (y_i - y_j)^2}$  is the separation between particles  $i$  and  $j$ , and  $\omega_x$  and  $\omega_y$  are the single-particle oscillation frequencies in the  $x$  and  $y$  directions, respectively. The equilibrium configuration minimizes  $U$ .

We nondimensionalize Eq. (2) using the variables  $\xi_i = x_i/r_0$ ,  $\eta_i = y_i/r_0$ ,  $\rho_{ij} = r_{ij}/r_0$  and parameters

$$\alpha^2 = \frac{\omega_y^2}{\omega_x^2}, \quad \kappa = \frac{r_0}{\lambda_D}. \quad (3)$$

Here the characteristic length

$$r_0 = \left( \frac{2}{m\omega_x^2} \frac{q^2}{4\pi\epsilon_0} \right)^{1/3} \quad (4)$$

is defined using the longitudinal frequency  $\omega_x$ . The dimensionless potential energy is then

$$\frac{U}{U_0} = \sum_{i=1}^n (\xi_i^2 + \alpha^2 \eta_i^2) + \sum_{i=1}^n \sum_{j>i}^n \frac{e^{-\kappa\rho_{ij}}}{\rho_{ij}}, \quad (5)$$

where  $U_0$  is the characteristic potential energy. Equilibrium configurations  $\{\eta_i, \xi_i\}$  of the model [Eq. (5)] depend on three parameters:  $n$ ,  $\kappa$  and  $\alpha^2$ . Here  $\kappa$  is the Debye shielding parameter and  $\kappa = 0$  corresponds to an unshielded Coulomb interaction. The well anisotropy parameter is  $\alpha^2$ . We assume  $\omega_y \geq \omega_x$  or  $\alpha^2 \geq 1$ . Straight line configurations  $y_i = \eta_i = 0$  then lie in the  $x$  (longitudinal) direction and are independent of  $\alpha^2$ . An equilibrium configuration  $\{\xi_i, \eta_i\}$  can be compared to an experimentally measured configuration  $\{x_i, y_i\}$  by multiplying each coordinate by  $r_0$ .

Within the context of this model [Eq. (5)], abrupt 1D to 2D transitions [10, 16] are predicted to occur for critical values of the three parameters  $n$ ,  $\kappa$  and  $\alpha^2$  due to a zigzag instability. This has been confirmed experimentally as  $n$  was varied by Melzer [11] and Sheridan and Wells [16]. Melzer [11] also observed a zigzag transition as the neutral gas pressure was changed, which presumably changed the plasma density and therefore both  $\kappa$  and  $\alpha^2$ . Sheridan and Wells [16] confirmed that the zigzag transition caused by increasing  $n$  in small clusters behaves as a continuous phase transition between 1D and 2D states, where the cluster width near the transition obeys a power law. Using the model of Eq. (5), they also predicted [16] that the zigzag transition in small clusters exhibits power law behavior as either  $\kappa$  or  $\alpha^2$  is varied. Piacente, et al. [17] reached a similar conclusion from a computational study of unbounded Yukawa systems ( $n \rightarrow \infty$ ) with a transverse parabolic well and longitudinal periodic boundaries. Structural transitions due to changes in  $\kappa$  or  $\alpha^2$  have not been characterized experimentally.

In this work we investigate the transitions a Yukawa cluster (i.e., a small dusty plasma) undergoes as the well anisotropy  $\alpha^2$  is varied. We use a novel experimental method in which the physical geometry of the confining potential well is changed without disrupting the plasma discharge. The discharge parameters are nearly constant, so that the Debye shielding parameter  $\kappa$  is also nearly constant. The well anisotropy is accurately determined using measured center-of-mass frequencies for the dusty plasma. As predicted [16], the transverse

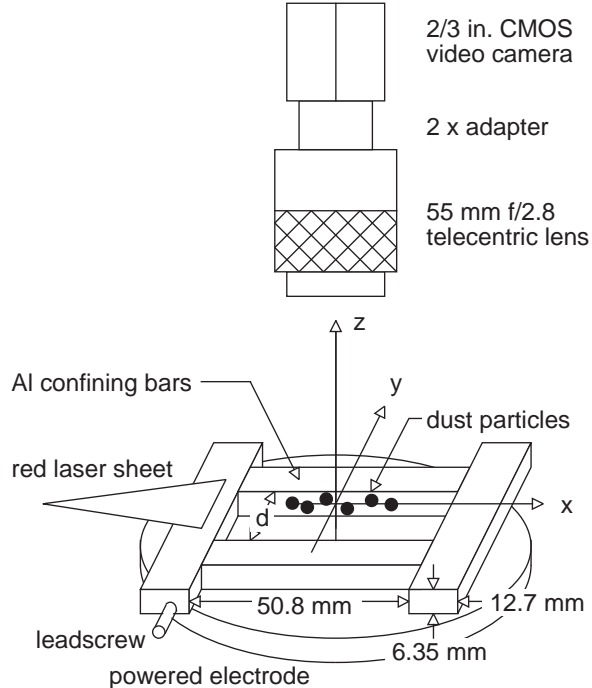


Figure 1: Schematic of the experimental geometry (not to scale). Six dust particles are confined in the biharmonic potential well created by a rectangular depression placed on the powered electrode in an rf discharge. The confining well anisotropy is varied by changing the width  $d$  while the plasma is on, and without losing the particles, using a lead screw.

cluster width  $y_{rms}$  exhibits power law behavior vs  $\alpha^2$  following the zigzag transition. The Debye shielding parameter is found by comparison to the model, and Debye shielding is shown to be important.

The dusty plasma was studied in the DONUT (Dusty Ohio Northern University experiment) apparatus (Fig. 1) [7, 8, 12, 16, 18, 19]. Argon gas was leaked into the vacuum chamber and the pressure was stabilized at 15.4 mtorr. At this pressure normal modes of the dust clusters are under damped [18]. Inside the chamber a capacitively-coupled rf electrode is used both to sustain the discharge and to levitate the dust particles. The rf frequency was 13.56 MHz, the forward rf power was  $\sim 7$  W and the dc self-bias on the electrode was  $-90$  V.

The confining well (Fig. 1) is produced by a rectangular aperture placed on the 89-mm diameter aluminum electrode, creating a biharmonic well in the horizontal ( $x$ - $y$ ) plane [3]. The aperture is made of four aluminum bars, each with a cross section of  $6.35$  mm  $\times$   $12.7$  mm. The depth of the trap is 6.35 mm, the length is fixed at 50.8 mm, and the width  $d$  is adjustable

from  $\approx 0$  to 38 mm. Here  $d$  can be adjusted while the plasma is on, and without losing the dust particles, by mean of a lead screw which is rotated from outside the vacuum. The lead screw is made of joined left-handed and right-handed threaded rods [unified national coarse (UNC) thread size 6-32] that move the two confining bars simultaneously closer together or farther apart a distance of 1/16 inch ( $\approx 1.59$  mm) per revolution, thus keeping the minimum of the potential well centered with respect to the disk electrode. This arrangement allows us to continuously vary the anisotropy parameter  $\alpha^2$  while maintaining nearly the same plasma discharge parameters.

The dust particles used were melamine formaldehyde resin spheres with a nominal diameter of  $9.62 \pm 0.09$   $\mu\text{m}$ . As noted previously [18], we believe that the particle diameter is actually 8.94  $\mu\text{m}$ , giving  $m = 5.65 \times 10^{-13}$  kg. Confined dust particles are illuminated by a red diode laser sheet. A top-view camera mounted about 30 cm above the electrode is used to acquire dust particle position data. For this experiment, the resolution of the camera and associated optics was 16.47  $\mu\text{m}/\text{pixel}$ . Sequences of 2048 frames were recorded at 27.9 frames/s. A side-view camera was used to confirm that there were no out-of-plane particles. We acquired 20 data sets with the same  $n = 6$  particles for trap widths  $d = 12.8$  to 36.6 mm.

Representative measured configurations are shown in Fig. 2 for increasing  $d$ . As seen in Fig. 2(a), the particles are in a straight line configuration when  $d$  is small, or equivalently,  $\alpha^2$  is large. As we increase  $d$  the cluster goes through two structural transitions, straight line to zigzag [Figs. 2(b) and (c)], and then zigzag to elliptical [Fig. 2(d)]. The transition to the zigzag state occurs at  $d \approx 23$  mm and the transition to the elliptical state occurs at  $d \approx 30$  mm. In the elliptical state all six particles lie on the convex hull of the cluster.

To analyze the experimental data, we first find the dependence of the anisotropy parameter  $\alpha^2$  on  $d$ . This is done by measuring the frequencies  $\omega_x$  and  $\omega_y$  of the c.m. modes from the particles' Brownian motions [8, 12, 16]. The power spectra of the time histories of the c.m. coordinates,  $x_{cm} = (1/n) \sum x_i$  and  $y_{cm} = (1/n) \sum y_i$ , were fitted with the expression for a driven damped harmonic oscillator to determine the corresponding normal mode frequencies  $\omega_x$  and  $\omega_y$ . For each  $d$ , the dust particle configuration was characterized by the root-mean-squared values  $x_{rms}$  and  $y_{rms}$  averaged over all frames, where

$$x_{rms}^2 = \frac{1}{n} \sum_{i=1}^n (x_i - x_{cm})^2, \quad y_{rms}^2 = \frac{1}{n} \sum_{i=1}^n (y_i - y_{cm})^2. \quad (6)$$

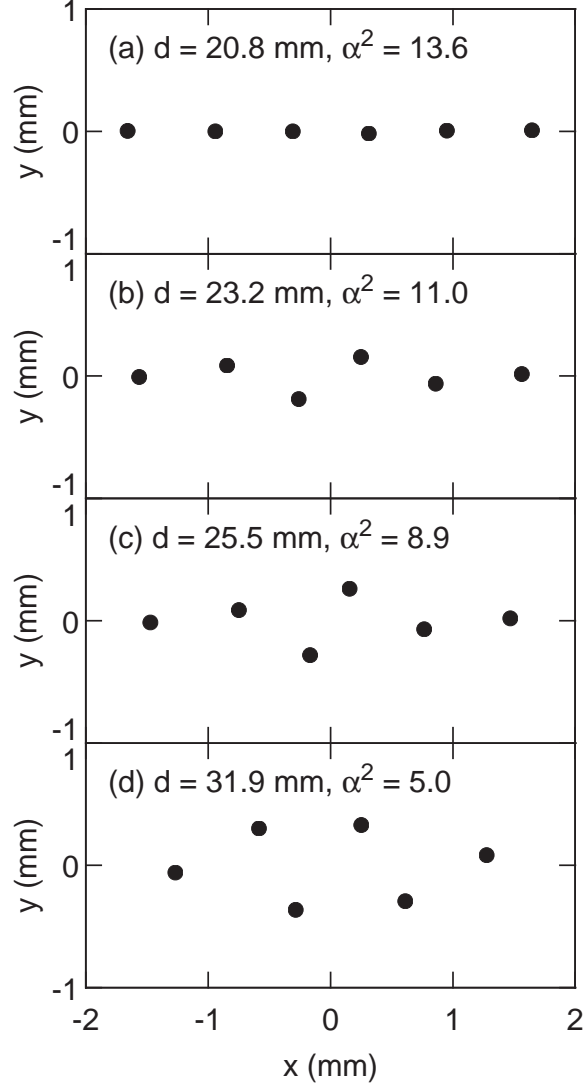


Figure 2: Measured particle configurations vs increasing trap width  $d$ , or equivalently, decreasing well anisotropy  $\alpha^2$ . (a) Straight line configuration, (b) and (c) zigzag configurations and (d) elliptical configuration. Values of the anisotropy parameter  $\alpha^2$  were determined from measured c.m. frequencies.

Here  $x_{rms}$  represents the longitudinal cluster size (i.e., its length), while  $y_{rms}$  is the transverse cluster width. In particular,  $y_{rms}$  can be used as an order parameter for the zigzag transition since  $y_{rms} = 0$  in the 1D straight line configuration and  $y_{rms} > 0$  for the 2D zigzag configuration [16].

The measured c.m. frequencies  $\omega_x$  and  $\omega_y$  are plotted vs  $d$  in Fig. 3(a). Here  $\omega_x$  (the frequency associated with the fixed 50.8 mm separation) shows a weak linear increase with

$d$ , while  $\omega_y$  is roughly constant for  $d \lesssim 20$  mm and then decreases as  $d$  increases. That is, for these experimental conditions decreasing  $d$  below  $\approx 20$  mm does not increase  $\omega_y$  because the sheath edge can no longer conform to the rectangular depression, but rather, is pushed upward [11]. This explanation is given further weight by measurements of the cluster height  $h$  above the top of the confining bars [Fig. 3(a)]. Here  $h$  was determined by the height of the laser sheet used to illuminate the particles and has an uncertainty  $\pm 0.2$  mm. As  $d$  increases  $h$  decreases, indicating that the sheath edge is moving into the rectangular depression.

Rather than taking  $\omega_x$  and  $\omega_y$  for each  $d$  and directly calculating  $\alpha^2$ , we fitted a line to  $\omega_x$  and a quadratic curve to  $\omega_y$  for  $d > 20$  mm, which spans the zigzag and elliptical transitions. The average value of  $\omega_x$  over this range is 7.47 rad/s. By dividing the two fitted curves we determined  $\alpha^2$  as a function of  $d$  [Fig. 3(b)]. We cover a wide range of anisotropies, where  $\alpha^2$  decreases with increasing  $d$  from  $\alpha^2 \approx 14$  to 2.5. If we could increase  $d$  to 50.8 mm to achieve an isotropic well, we would expect  $\alpha^2 = 1$ . The slight increase of  $\omega_x$  with  $d$  implies that  $\kappa \propto \omega_x^{-2/3}$  increases weakly with  $\alpha^2$ . If the only change in  $\kappa$  is due to  $\omega_x$ , then we estimate that  $\kappa$  increases by  $\approx 6\%$  over the range of  $\alpha^2$  values considered.

The measured cluster width  $y_{rms}$  and length  $x_{rms}$  are plotted vs  $\alpha^2$  in Figs. 4(a) and (b), respectively. From the  $y_{rms}$  data we observe a transition from the 1D configuration to a 2D zigzag configuration at  $\alpha^2 \approx 12$ . From  $\alpha^2 \approx 12$  to 6.5, the  $y_{rms}$  data is well fitted by a power law with a critical value  $\alpha_c^2 = 12.1$  and an exponent of 0.35. The model solution shows the same power law behavior [16]. The divergence from the power law fit at  $\alpha^2 \lesssim 6.5$  indicates a second transition [16], from the zigzag configuration to an elliptical configuration. The elliptical structure [12] occurs when the second (fifth) particle in the cluster moves between the first and third (fourth and sixth) particles, thereby moving onto the convex hull of the cluster. Since the equilibrium shell structure for six particles in an isotropic well is (1, 5), a further symmetry breaking transition is needed to reach the  $\alpha^2 = 1$  configuration.

For the first value of  $d$  after the zigzag transition ( $\alpha^2 = 11.8$ ), the cluster was seen to flip between the two anti-symmetric zigzag configurations. (Since we can vary  $\alpha^2$  continuously it is possible to tune for this behavior.) A zigzag configuration has two degenerate states since the energy is invariant under a reflection of particle coordinates  $y \rightarrow -y$ . In a stable zigzag configuration these two states are separated by a potential barrier corresponding to the higher energy of the unstable straight line configuration and the zigzag state is bistable. Just above the zigzag transition the barrier between the two states is low, and thermal

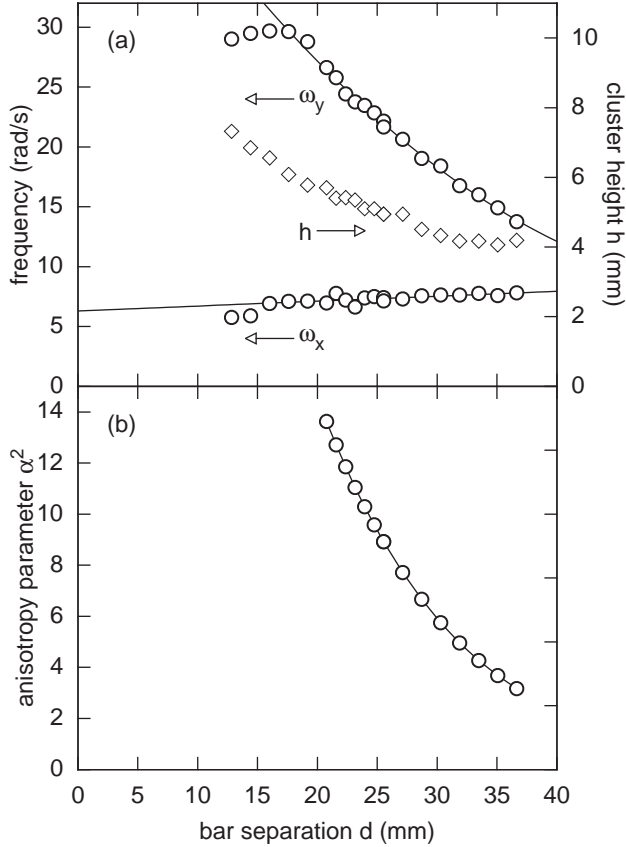


Figure 3: (a) Dependence of measured c.m. frequencies  $\omega_x$  and  $\omega_y$  and the height  $h$  of the cluster above the top of the well on the width  $d$ . Here  $\omega_x$  is fitted with a linear function and  $\omega_y$  with a quadratic curve. (b) Dependence of the smoothed anisotropy parameter  $\alpha^2 = \omega_y^2/\omega_x^2$  on  $d$ .

fluctuations or small periodic perturbations can cause the system to flip between the two zigzag states, as was observed. For the next lower value of  $\alpha^2$  flipping was not seen, indicating that the potential barrier between the two degenerate zigzag states was then too high.

Theoretical configurations which can be compared to the experiment are found by minimizing Eq. (5), allowing us to predict  $x_{rms} = r_0 \xi_{rms}$  and  $y_{rms} = r_0 \eta_{rms}$  as a function of  $\alpha^2$ . To calculate a configuration three parameters,  $\alpha^2$ ,  $\kappa$  and  $n$ , are required. We know  $n$ , and  $\alpha^2$  has been measured, so we only need to determine the shielding parameter  $\kappa$ . To do this we assume that  $\kappa$  is independent of  $\alpha^2$  and then minimize the sum of the squared differences between the measured and computed values of  $y_{rms}$ , giving  $\kappa = 2.4$  and  $r_0 = 1.25$  mm. The Debye length  $\lambda_D = r_0/\kappa = 0.52$  mm is comparable to the inter-particle distance and the average charge  $q = -1.2 \times 10^4 e$ . These values are consistent with those found in previous experiments for similar plasma conditions [8, 12, 16, 18, 19].



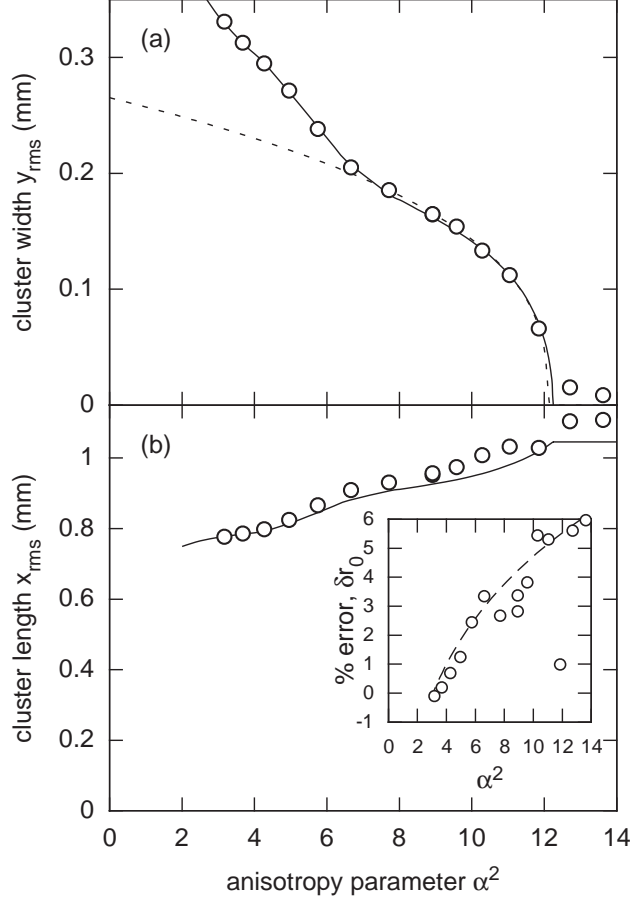


Figure 4: (a) Measured cluster width  $y_{rms}$  (open circles), power law fit to data near the zigzag transition (dashed line) and widths computed from the model for  $\kappa = 2.4$  and  $r_0 = 1.25$  mm (solid line) vs the measured anisotropy parameter  $\alpha^2$ . (b) Measured cluster length  $x_{rms}$  (open circles) and lengths computed from the model (solid line) vs  $\alpha^2$ . (Inset) Comparison of the percentage difference between the  $x_{rms}$  data and the model (open circles) with the percentage change in  $r_0 \sim \omega_x^{-2/3}$  (broken line) vs  $\alpha^2$ .

As shown in Fig. 4(a), the cluster width  $y_{rms}$  calculated using the model for  $\kappa = 2.4$  and  $r_0 = 1.25$  mm exhibits excellent agreement with the experimental data, including reproducing the transition between the zigzag and elliptical configurations. The agreement between the measured and predicted values of  $x_{rms}$  provides a cross check on the model. We find that the predicted values of  $x_{rms}$  [Fig. 4(b)] show good agreement for  $\alpha^2 \lesssim 4$ , but systematically underestimate the measured cluster length as  $\alpha^2$  increases. For the longest clusters, which are in a straight line configuration, the predicted cluster lengths are about 6% below

the measured values. As shown in the Fig. 4(inset), this difference can be attributed to an experimental increase in  $r_0 \sim \omega_x^{-2/3}$  due to the measured decrease of  $\omega_x$  with  $\alpha^2$ . This implies that the average particle charge  $q$  is effectively constant, as previously observed for constant neutral pressure [8, 19]. This increase in  $r_0$  with  $\alpha^2$  is not as apparent for  $y_{rms}$  since  $y_{rms} \lesssim 0.2x_{rms}$  and  $y_{rms} \rightarrow 0$  as  $\alpha^2$  increases.

In summary, we have provided direct evidence that the width of a Yukawa cluster exhibits power law behavior for the 1D to 2D zigzag transition caused by decreasing the confining well anisotropy parameter  $\alpha^2$ , confirming a previous prediction [16]. Experiments were performed using a dusty plasma with  $n = 6$  particles confined in the biharmonic well above a rectangular depression. The width  $d$  of the rectangular depression was increased while the plasma remained on to decrease  $\alpha^2$  while the Debye shielding parameter  $\kappa$  remained essentially constant. The dependence of  $\alpha^2$  on  $d$  was accurately determined by measuring the c.m. frequencies of the dusty plasma. A transition from the zigzag configuration to an elliptical configuration was also observed. The cluster width was found to be in excellent agreement with the predictions of a model which assumes identical particles confined in a 2D biharmonic well and interacting through a Yukawa potential. From the fit to the model we found the Debye length is comparable to the inter-particle distance, so that Debye shielding significantly effects the physics of these clusters.

## Acknowledgments

Portions of this paper are taken from A. L. M.'s undergraduate physics thesis.

- 
- [1] F. F. Chen, Introduction to Plasma Physics (Plenum, New York, 1974), p. 3.
  - [2] M. Lampe, G. Joyce, G. Ganguli and V. Gavrishchaka, Phys. Plasmas **7**, 3851 (2000).
  - [3] A. Homann, A. Melzer, S. Peters and A. Piel, Phys. Rev. E **56**, 7138 (1997).
  - [4] T. Misawa, N. Ohno, K. Asano, M. Sawai, S. Takamura and P. K. Kaw, Phys. Rev. Lett. **86**, 1219 (2001).
  - [5] B. Liu and J. Goree, Phys. Rev. E **71**, 046410 (2005).
  - [6] W.-T. Juan, Z.-H. Huang, J.-W. Hsu, Y.-J. Lai and L. I, Phys. Rev. E **58**, R6947 (1998).
  - [7] T. E. Sheridan, J. Phys. D: Appl. Phys **39**, 693 (2006).

- [8] T. E. Sheridan and W. L. Theisen, *Phys. Plasmas* **13**, 062110 (2006).
- [9] O. Arp, D. Block, A. Piel and A. Melzer, *Phys. Rev. Lett.* **93**, 165004 (2004).
- [10] L. Cândido, J.-P. Rino, N. Studart and F. M. Peeters, *J. Phys.: Condens. Matter* **10**, 11627 (1998).
- [11] A. Melzer, *Phys. Rev. E* **73**, 056404 (2006).
- [12] T. E. Sheridan, K. D. Wells, M. J. Garee and A. C. Herrick, *J. Appl. Phys.* **101**, 113309 (2007).
- [13] J. P. Schiffer, *Phys. Rev. Lett.* **70**, 818 (1993).
- [14] S. W. S. Apolinario, B. Partoens and F. M. Peeters, *Phys. Rev. E* **74**, 031107 (2006).
- [15] T. E. Sheridan, *Phys. Scr.* **80**, 065502 (2009).
- [16] T. E. Sheridan and K. D. Wells, *Phys. Rev. E* (in press).
- [17] B. Piacente, I. V. Schweigert, J. J. Betouras and F. M. Peeters, *Phys. Rev. B* **69**, 045324 (2004).
- [18] T. E. Sheridan, *Phys. Rev. E* **72**, 026405 (2005).
- [19] T. E. Sheridan, *J. Appl. Phys.* **106**, 033303 (2009).